FRACTOGRAPHIC OBSERVATIONS ON STRESS CORROSION CRACKING OF SOME FACE-CENTRED-CUBIC ALLOYS

H. E. Hänninen, J. A. Honkasalo and H. A. A. Pitkänen*

INTRODUCTION

The deformation microstructure of alloys which are susceptible to stress corrosion cracking (SCC) has been shown to affect strongly the mode of failure in face-centred-cubic metals [1]. Alloys with a low stacking fault energy (SFE) containing planar groups of dislocations are generally more prone to transgranular SCC, whereas alloys of higher SFE normally exhibit intergranular SCC. Fractography of 304L type austenitic stainless steel in boiling $MgCl_2$ solutions [2-4] and in H_2SO_4/NaCl environments at ambient temperature [5,6] has been studied in detail. However, only few fractographical examinations have been made by scanning electron microscopy (SEM) to determine, whether the same mechanism of SCC is applicable to transgranular fracture of low SFE alloys as 304L type austenitic stainless steel, α-brass and α-Cu-Al alloys in contact with different corrosive environments.

EXPERIMENTAL METHODS

The test materials were AISI 304L type austenitic stainless steel (C 0,03, Cr 18,6 and Ni 10,9), α-brass (Cu-37Zn and Cu-20Zn) and α-Cu-Al alloys containing 3,5% and 6% Al. These alloys are known to have low SFE, planar deformation microstructure and similar physical and mechanical properties. 304L steel specimen measuring 1.5x16x140 mm for long term SCC test without applied tensile stress in boiling $MgCl_2$ solution and specimens tested in HCl and NaCl solutions were annealed for 75 h at 1423 K. Cu-37Zn and Cu-20Zn specimens were annealed for 4 h at 743 K and 1023 K, respectively. α-Cu-Al alloys were manufactured using a graphite crucible in a protective atmosphere. Each alloy was melted twice in order to achieve as homogeneous a structure as possible. After cold rolling the specimens were annealed at 873 K for 23 h. All anneals were carried out in evacuated silica tubes, and specimens were then air cooled to minimize the residual stresses. After heat treatment flat 304L steel specimen was slightly pickled by HNO_3-HF mixed acid solution, while the surfaces of other specimens were electropolished. SCC experiments of 304L steel and α-brass were performed with specimens, measuring 1.5x10x70 mm. All the specimens, except those used without applied stress, were U-bent in the same way to a radius of 9 mm. After bending, the specimens were pressed into holders made of the same material. The size of the U-bend specimens of α-Cu-Al alloys was 0.5x5x30 mm, the radius of the bend was 4 mm and the specimen holder was a simple teflon stressing rig. 304L steel and Cu-alloys were tested in their specific environments, Table 1. Specimens were immersed completely in the solutions or in the case of NH_3 atmosphere they were kept in vapour 5 cm above the surface of the solution. After the corrosion tests specimens were rinsed with water and ethanol and examined in the SEM in conjunction with the X-ray microanalyzer.

*Helsinki University of Technology.

RESULTS

The main emphasis was on the propagation of stress corrosion cracks, although nucleation was also examined in some cases. Attention has been paid to common features of fractographs characterizing the SCC of each alloy.

Austenitic Stainless Steels

Fracture of 304L type austenitic stainless steel has been examined in three different environments: 1.5 N HCl at room temperature, NaCl solution boiling at 382 K and $MgCl_2$ solution boiling at 408 K.

In 1.5 N HCl solution SCC initiates mainly as a consequence of selective dissolution at grain boundaries on the tensile surface of the U-bend specimens, but immediately beneath the outer layer transgranular cracks are developed. Figure 1(a) shows the outer surface of the specimen. A considerable attack has occurred at grain boundaries and also at coherent and non-coherent twin boundaries. However, the amount of general corrosion seems to be slight. In Figure 1(b) the nucleation of transgranular fracture from the grain boundary is seen to occur by multiple crack nucleation where cracks propagate on a number of parallel planes but later their number decreases. A row of round pits (tunnels) can be detected at the grain boundary (A), where the cracks have initiated. The measured diameter of the pits is about 1 μ, which agrees very well with the results of Harston and Scully [5] in H_2SO_4/NaCl environments and is also of the same order of magnitude as pits measured by Scamans [7] in thin foil tensile specimens using 0.5 M HCl solution at 298 K. On the fracture surface signs of general corrosion (B) can also be seen, but it is difficult to say whether or not this attack has occurred after the fracture surface has formed. The fan-shaped pattern of this fractograph is evident and it is very similar to those normally produced in boiling $MgCl_2$ solutions. Figure 1(c) illustrates another view of the nucleation of fracture showing initiation from a grain boundary (C) as well as directly from the outer surface (D). The effect of grain boundaries on the propagation of fracture is shown clearly in this fractograph; the stepped structure seems to originate mainly from the grain boundaries. A small area of intergranular cracking can also be observed. Planar selective dissolution on the fracture surface can be seen in Figure 1(d) which is a detail of Figure 1(c). The tunnel-like attack is very clearly visible. No corrosion products can be observed in connection with tunnel formation.

In boiling NaCl solution SCC is transgranular; no intergranular separation was detected, while a mixed mode of fracture can be detected in $MgCl_2$ quite often [4]. The morphology of the fracture surface in NaCl is very similar to that seen in fractographs using HCl solution, with the exception of minor traces of selective and general dissolution. In Figure 2(a) a typical fan-shaped fractograph can be seen. Figures 2(b) and 2(c) show close matching of opposite fracture surfaces, where the change of fracture path at twin boundaries and fine, parallel secondary microcracks can be detected.

In boiling $MgCl_2$ solutions SCC can also be developed without applied stress. Figure 2(d) shows a typical SCC fracture surface of 22.5 % pre-strained 304L steel after exposure for 721 h in at 408 K boiling $MgCl_2$ solution, where the change of fracture path at twin boundaries can be detected. Nielsen [8], however, has shown that transgranular SCC can also develop in similar long term test in unnotched initially fully annealed

304L steel, which has the typical SCC fracture surface as previously shown by Hänninen and Honkasalo [4]. In these specimens residual stresses, if there exists any, are so minor that only source of stresses must be the corrosion process itself.

α-Brass and α-Cu-Al Alloys

Cu-20Zn normally cracks completely intergranularly. Intergranular separation was also observed in fully annealed tensile specimens after exposure for 240 h in NH_3 atmosphere without any applied external stress, as shown in Figure 3(a). On the intergranular fracture surface signs of localized corrosion can be detected near the outer surface. Figure 3(b) shows a detail of a tetrahedron-like corrosion pit on the intergranular fracture surface. It can be deduced from the slip traces which are formed during straining to fracture in a tensile testing machine after the corrosion test that the walls of this faceted pit are {111} planes. On the fracture surface, which is visually yellow, there is a continuous transparent film which has broken in the area of the pit. The morphology of larger area of crystallographic type of pitting is illustrated in Figure 3(c). The corrosion product left on the area (A) was found to consist only of Cu-compounds. On the intergranular fracture surface there was no evidence of markings resulting from the discontinuous crack propagation.

In Figure 4(a) the nucleation of SCC in Cu-37Zn in NH_3 atmosphere can be observed. On the outer surface an aggregate of small platelets forming thick (approx. 5 μm), dark tarnish oxide film and on the fracture surface a different type of corrosion product can be detected. Electron microprobe analysis indicated that the thick tarnish film is essentially depleted with respect to Zn, while the corrosion product on the fracture surface contains only Zn. However, the amount of this Zn-rich corrosion product on the fracture surface decreases and it finally disappears at the crack tip. Visually the outer surface of the specimen is dark and the fracture surface is yellow. Figures 4(b) and 4(c) show typical transgranular SCC morphology of matching opposite fracture surfaces of Cu-37Zn in NH_3 atmosphere.

Figure 5(a) shows an example of a fracture surface of Cu-37Zn produced in 12.5 % NH_3 solution after 500 h exposure. The fracture surface shows much finer morphology than in other samples, but the stepped structure originating from the grain boundary is also in this case very clear. Figures 5(b) and 5(c) present fractographs produced in Mattsson's solution. The stepped character in both fractographs is evident. Figure 5(c) shows the generation of steps from the grain boundary indicating a very clear saw-tooth structure. Especially these two fractographs of α-brass resemble very closely Nielsen's replicas [8] of SCC fracture surfaces of austenitic stainless steels cracked in boiling $MgCl_2$ solution as well as some fracture surfaces in close-packed-hexagonal Mg-7.5Al alloy tested at room temperature in an aqueous NaCl-K_2CrO_4, as shown by Chakrapani and Pugh [9].

This corrosion product film which formed in NH_3 atmosphere on the fracture surfaces of α-Cu-Al alloys made the study of fracture surface morphology of these alloys rather difficult. Figure 6(a) shows a part of the fracture surface of Cu-6Al alloy after 325 h exposure to 25 % NH_3 atmosphere having very similar saw-tooth morphology as could be seen in Cu-37Zn. Figure 6(b) shows the change from intergranular to transgranular mode of fracture and in Figure 6(c) is shown a part of the intergranularly

separated fracture surface where also localized selective corrosion on slip traces has occurred. Cu-3.5Al alloy cracked completely intergranularly.

DISCUSSION

The following common features have been found in this fractographical investigation of three different alloys in different environments:

- The transgranular crack path changes its direction at grain boundaries and at twin boundaries having a stepped morphology which is common to all the studied alloys. However, there are some differences in the detailed morphology of the steps (the saw-tooth profile is more prominent in Cu-alloys). Opposite fracture surfaces show also very detailed matching.
- Transgranular and intergranular fracture depends on the composition of these alloys; transgranular fracture, however, is predominant.
- External applied stress was found to be not a necessary requirement for the intergranular SCC to occur in Cu-20Zn. This was also found to be true with austenitic stainless steels, where the cracks are, however, transgranular [4,8].
- Deposited corrosion products on the fracture surface were only detected in Cu-alloys.

These observations, in spite of that SEM fractographic observations are not sufficient to determine the mechanism of SCC, are in agreement with the hypothesis that these alloys which have similar physical and mechanical properties, despite of different environments and dissolution kinetics, have likely a common mechanism of SCC. If this is so, we can draw the following conclusions concerning the theories of SCC:

- The SCC theory, in which a martensite transformation provides an active path for SCC [10] is out of the question, because in Cu-alloys used in this study there is not such a transformation.
- Crack propagation by successive slip step dissolution [11] is also thought to be unlikely, because the SCC fracture surfaces are brittle in nature and minor traces of corrosion can normally be observed. A close matching of opposite fracture surfaces is observed, too. In HCl solution stainless steel is in the active state and no oxide film exists in the crack tip. This mechanism involves plastic deformation at the crack tip, but cracking was also observed without external applied stress.
- The tarnish rupture mechanism for Cu-alloys is also unlikely, because the thick, dark tarnish film covers only the outer surfaces. The yellow fracture surface was observed to be covered by a very thin and possibly a more protective film which has been demonstrated to be of Cu_2O [12].

ACKNOWLEDGMENTS

The authors wish to thank Professor V. K. Lindroos for his encouragement and for providing experimental facilities. Thanks are also due to Mr. P. Pitcher for correcting the English text. This research was supported in part by the Foundation of Outokumpu Company.

REFERENCES

1. SWANN, P. R., Corrosion, 19, 1963, 102t.
2. HARSTON, J. D. and SCULLY, J. C., Corrosion, 26, 1970, 387.
3. SCULLY, J. C., The Theory of Stress Corrosion Cracking in Alloys, NATO, Brussels, 1971, 125.
4. HÄNNINEN, H. E. and HONKASALO, J. A., 6th International Congress on Metallic Corrosion, Sydney, 1975.
5. HARSTON, J. D. and SCULLY, J. C., Corrosion, 25, 1969, 493.
6. HONKASALO, J. A. and HAKKARAINEN, T. J., Scand. J. Met., 4, 1975, 185.
7. SCAMANS, G. M., PhD Thesis, University of London, 1973.
8. NIELSEN, N. A., J. Mater., 5, 1970, 794.
9. CHAKRAPANI, D. G. and PUGH, E. N., Met. Trans., A6, 1975, 1155.
10. BIRLEY, S. S. and TROMANS, D., Corrosion, 27, 1971, 63.
11. STAEHLE, R. W., ref. 3, 223.
12. BIRLEY, S. S. and TROMANS, D., Corrosion, 27, 1971, 297.

Table 1 Test Environments

Material	Environment	Concentration	Temperature	pH
304L	HCl	1,5 N	Ambient	0,0±0,5
304L	NaCl	Saturated	Boil. at 382 K	-
304L	$MgCl_2$	38 wt %	Boil. at 408 K	1,5±0,5
Cu-20Zn	NH_3, vapour	12,5 %	Ambient	-
Cu-37Zn	NH_3, vapour	12,5 %	Ambient	-
Cu-37Zn	NH_3	12,5 %	Ambient	11,5±0,5
Cu-37Zn	Mattsson's sol.	-	Ambient	11,0±0,5
Cu-6Al	NH_3, vapour	25 %	Ambient	-
Cu-3,5Al	NH_3, vapour	25 %	Ambient	-

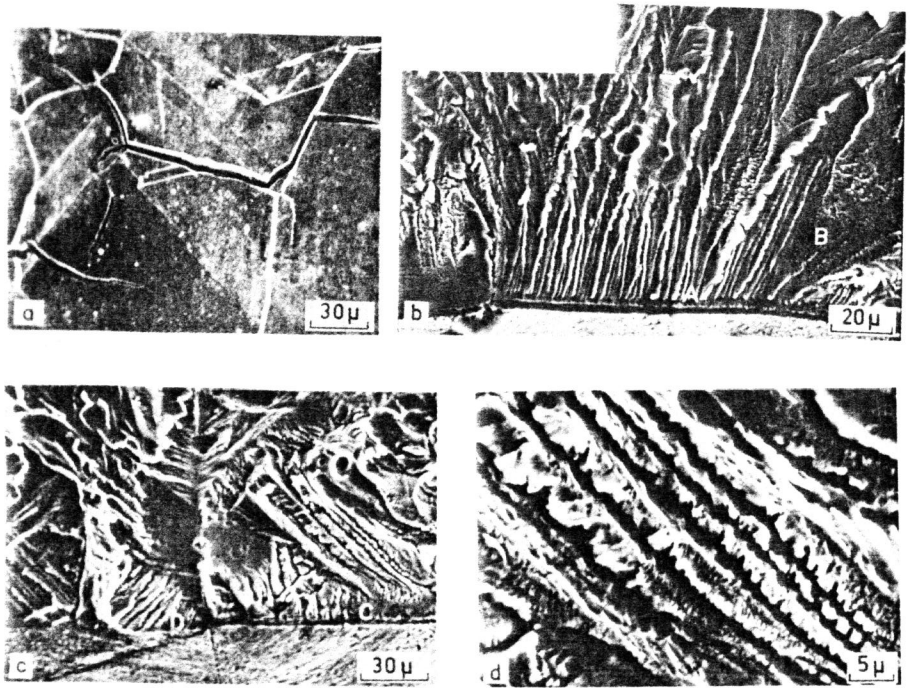

Figure 1 (a) Outer Surface of 304L Steel after 310 h Exposure to 1.5 HCl
(b) Initiation of Transgranular SCC from the Grain Boundary Groove
(c) Fractograph Illustrating a Further Example of Nucleation
(d) Detail of the Selective Dissolution on the Fracture Surface

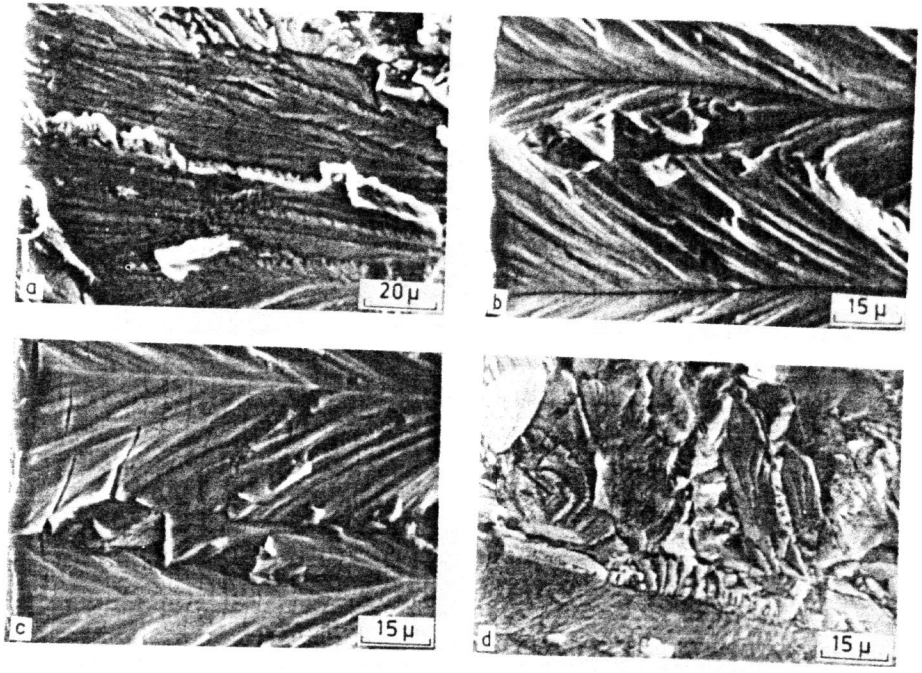

Figure 2 (a) Fractograph of 304L Steel after 1125 h Exposure to Boiling NaCl at 382 K
(b) and (c) Opposite Fracture Surfaces of the Same Specimen
(d) SCC Fracture Surface of 22.5% Prestrained 304L Steel After 721 h Exposure to Boiling $MgCl_2$ at 408 K without External Applied Stress

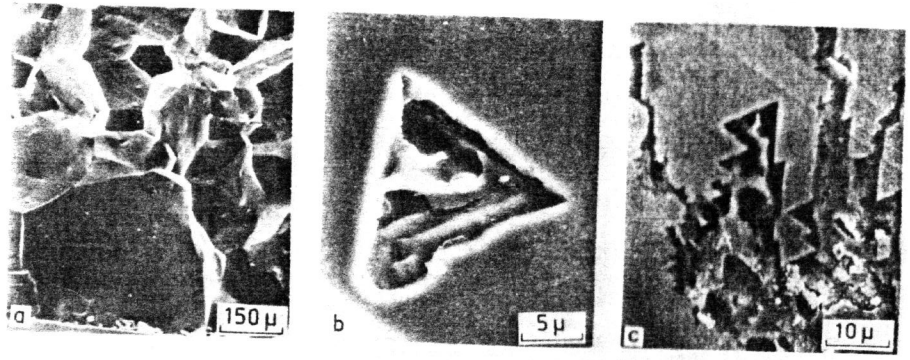

Figure 3 (a) Intergranular Fracture Surface of Fully Annealed Cu-20Zn Obtained by Straining to Fracture after 240 h Exposure to NH_3 Atmosphere
(b) and (c) Details of Localized Corrosion on the Intergranular Fracture Surface

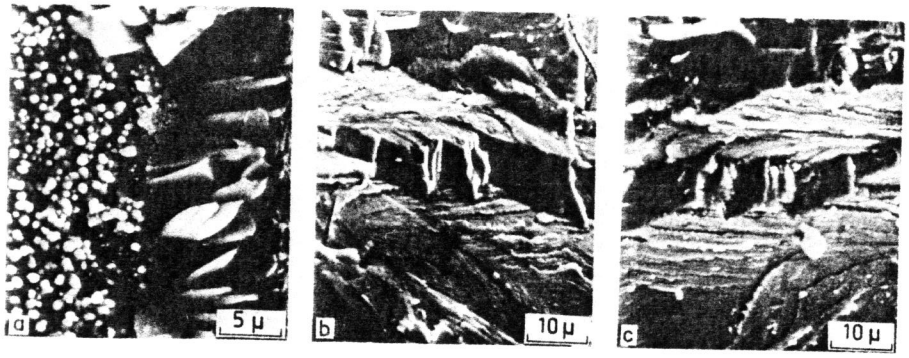

Figure 4 (a) Nucleation of SCC in Cu-37Zn after 22 h Exposure to NH_3 Atmosphere
(b) and (c) Opposite Fracture Surfaces of the Same Specimen

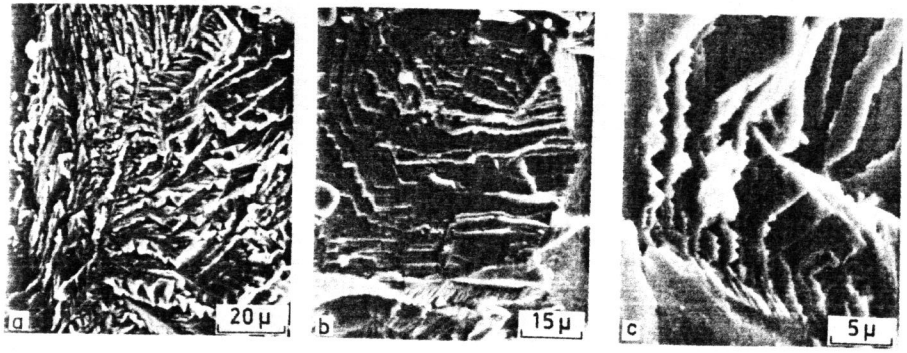

Figure 5 (a) Part of the Fracture Surface of Cu-37Zn after 500 h Exposure to 12.5% NH_3 Solution
(b) and (c) Typical Morphologies of Fracture Surfaces of Cu-37Zn after 95 h Exposure to Mattsson's Solution

Figure 6 (a), (b) and (c) Fractographs of Cu-6Al after 335 h Exposure to 25% NH_3 Atmosphere